Available online at www.sciencedirect.com
ScienceDirect
Journal of the European Ceramic Society 27 (2007) 2217–2222
www.elsevier.com/locate/jeurceramsoc

Effect of additives on the pore evolution of zirconia based ceramic foams after sintering

Tsuyoshi Higashiwada, Hiroshi Asaoka, Hidetaka Hayashi, Akira Kishimoto *

Division of Chemistry and Biochemistry, Graduate School of Natural Science and Technology, Okayama University, 3-1-1 Tsushima-Naka, Okayama 700-8530, Japan

Received 27 April 2006; received in revised form 26 July 2006; accepted 7 August 2006
Available online 25 September 2006

Abstract

A new superplasticity foaming method was used to form zirconia-based ceramic foams. Silica and alumina were chosen as additives because they facilitate the 2D superplastic deformation. The effects of these additives on macroscopic pore evolution were examined after heat treatment for up to 40 h. The addition of silica or alumina also enhanced the 3D deformation during superplasticity foaming. The total porosity of mono-foams made from 3 mol% yttria-stabilised zirconia without additives increased with heat treatment for up to 24 h, and then levelled off. The porosity of silica-dispersed foam was greater than that without additives and continued to increase for up to 40 h. Conversely, the porosity of alumina-dispersed ceramic foam reached saturation within 8 h. Consequently, the porosity of alumina-dispersed foam was greater than that without additives after heating for 8 h, while the latter exceeded the former with prolonged heating for more than 16 h. The detailed effects of alumina dispersion on the foam development behaviour were examined in connection with the microstructure.

Keywords: ZrO_2; Insulators; Superplasticity; Grain size; Porosity

1. Introduction

Given global demands, energy must be used effectively. Research has examined various ways to improve the performance of refractory materials to enhance the efficiency of power supplied by combustion.[1,2] Since the gaseous phase transmits little heat, the refractory materials used usually have a porous morphology. In addition to being good thermal insulators, structural reliability is also required for high-temperature refractory materials for the safe operation of power generators.

Practical candidates for high-temperature refractory materials are limited to oxide ceramics because of their high melting point and excellent oxidation durability. Since ceramic-based materials have other advantages, such as chemical stability and an abundance of raw starting materials, they are most suitable for use in the thermal insulation walls of industrial furnaces.

The foaming method is usually used to fabricate porous materials, which involves evaporating a foaming agent at near the melting point of the matrix. Polymer foams, such as polystyrene, are in widespread use, and both metal and glass foams have practical applications. However, the formation of ceramic foams at above their melting point (*e.g.*, 2720 °C for zirconia ceramics) has not proved practicable. Accordingly, conventional porous ceramics are usually fabricated by insufficient sintering using pore-forming agents.[3] Since sintering leads to the elimination of pores, sintering should not be completed in the fabrication of porous ceramics. Consequently, the inter-grain bonding of conventional porous ceramics is weak, resulting in a tremendous reduction in their mechanical strength. In addition, open pores predominate, which allows heat convection at higher temperatures, reducing the thermal insulating properties.

Recently, we developed a superplasticity foaming method to introduce pores after densification utilising superplasticity.[4,5] In our porous ceramics, the foaming processing is carried out after sintering; consequently, almost all of the pores are closed, with fully densified pore walls. The resulting ceramics have a high level of gas tightness and excellent thermal insulation, while maintaining their mechanical properties.

Previously, we reported the heating time-dependent porosity of superplasticity-foamed ceramics for up to 8 h, during

* Corresponding author. Tel.: +81 86 251 8069; fax: +81 86 251 8069.
E-mail address: kishim-a@cc.okayama-u.ac.jp (A. Kishimoto).

0955-2219/$ – see front matter © 2006 Elsevier Ltd. All rights reserved.
doi:10.1016/j.jeurceramsoc.2006.08.008

which the porosity of 3 mol% yttria-stabilised zirconia-based mono-foam continued to increase.[4] This indicates that the pores expand after densification. In this study, we prolonged the heating time for as long as 40 h and evaluated the evolution of macroscopic pores. In addition, we previously reported the preliminary results for mono-foams doped with silica, which facilitates superplasticity.[4] This study used another dispersoid, alumina, which also facilitates superplasticity, and we also examined the effect of such dispersoids on pore evolution in connection with the microstructure.

2. Experimental procedure

To demonstrate ceramic foaming following the sintering process, macroscopic single foams were fabricated using a method similar to that previously reported.[4,5]

In short, 3 mol% yttria-stabilised zirconia powder, denoted as 3YSZ (TZ-3Y, average grain size: 0.05 μm; Tosoh, Tokyo, Japan), was used as the matrix with and without dispersoids to enhance the superplasticity. Silicon carbide was used as a high-temperature foam agent that decomposes to evaporate at high temperatures. First, 0.1 g of silicon carbide powder (Grade-UF; Ibiden, Aichi, Japan) was pressed into a pellet in a Ø10-mm die under 30 MPa. Approximately 4 g of 3YSZ-based powder were weighed. In sequential order, half of the 3YSZ-based powder, the compressed silicon carbide powder, and the remaining half of the 3YSZ-based powder were put in a Ø20-mm steel die and pressed uniaxially at 30 MPa for 1 min, and then hydrostatically at 200 MPa for 1 min. The resultant powder compacts were heated to 1600 °C at a rate of 800 °C/h, kept at that temperature for 4–40 h, and then cooled. All the heat treatments were conducted in atmospheric ambient.

To evaluate the effects of the kind and amount of additives, the fabrication conditions other than the holding time were fixed, including the kind and amount of foaming agent, and the powder compaction and heating programs.

As additives to the 3YSZ matrix powder, alumina (AKP-30, average grain size: 0.4 μm; Sumitomo Chemical, Tokyo, Japan) and silica sol (Snow Tex S; Nissan Chemical, Tokyo, Japan) were tested. Each additive was mixed into 3YSZ powder with an atomic ratio of 10 mol% and wet ball milled using ethanol. After dried, each powder mixture was subjected into the powder compaction followed by heat treatment.

The external dimensions of the zirconia-based ceramic foams, such as foam height and foam diameter, were measured using caliper. The apparent density of the outer shell and of the entire ceramic foam was measured using Archimedes' method with water as the medium. The porosity of the ceramic foam was estimated from the apparent density of the ceramic foam and the relative density of the outer shell. To evaluate the grain size distribution, the fracture surface of the outer shell was polished with a 9-μm diamond paste, etched thermally at 1500 °C for 30 min, and examined under a scanning electron microscope (SEM). The sizes of approximately 100 ceramic grains were calculated using the code method and their distribution was evaluated. Crystalline phases that formed on the inner and outer sides of the shell were identified using an X-ray diffraction method (XRD) with Cu Kα radiation.

3. Results and discussion

Side views of the zirconia-based ceramic foams made using the superplasticity foaming method are shown in Fig. 1. The relative densities (*i.e.*, the ratio of the apparent density to the theoretical value) measured on the foam walls all exceeded 99% for 3YSZ-based foams without additives with heat treatment for up to 40 h. These results indicate that the densities of the once densified foam walls were maintained during pore evolution under these experimental conditions. For alumina- or silica-dispersed foams, the apparent density decreased slightly, while the relative density remained as high as 94%.

The total porosity of mono-foams fabricated from different matrices following the same thermal program or at 1600 °C with an 8-h hold, was in the order silica-dispersed > alumina-dispersed > without dispersoid. This tendency was consistent with the reported superplasticity property.[6]

While previous studies typically made use of the two-dimensional tensile condition, the addition of silica or alumina enhances the 3D deformation during superplasticity foaming in the present study. Therefore, the data obtained from the 2D tensile deformation test can be roughly applied to superplasticity foaming. Consequently, the heat-holding time could be reduced by considering the rapid superplastic deformation such as reported in spinel-dispersed YSZ.[7]

Furthermore, our superplasticity foaming method, which is compatible with the superplasticity deformation test, could be used as a simple gas pressure deformation test at high temperature. Foaming deformation is similar to superplasticity processing using gas pressure.

We examined the change in the total porosity of 3YSZ-based mono-foams with heating time for up to 40 h, which is plotted in Fig. 2. The porosity of mono-foams of 3YSZ without additives increased with heat treatment duration for up to 24 h, and then levelled off. Conversely, the porosity of alumina-dispersed ceramic foam almost saturated before 8 h, while that for silica-dispersed foam was greater than that without additives and continued to increase up to 40 h.

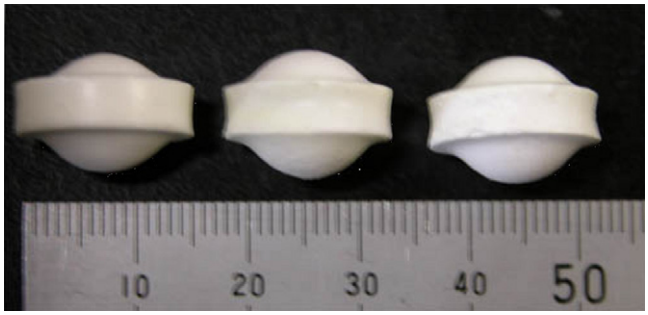

Fig. 1. Side view of macroscopic ceramic foams fabricated by foaming after sintering of zirconia based matrix with silicon carbide as a foam agent (1600 °C holding for 8 h). Foam height: 5.5 mm (left: 3YSZ), 6.5 mm (middle: silica added), 6.2 mm (right: alumina added).

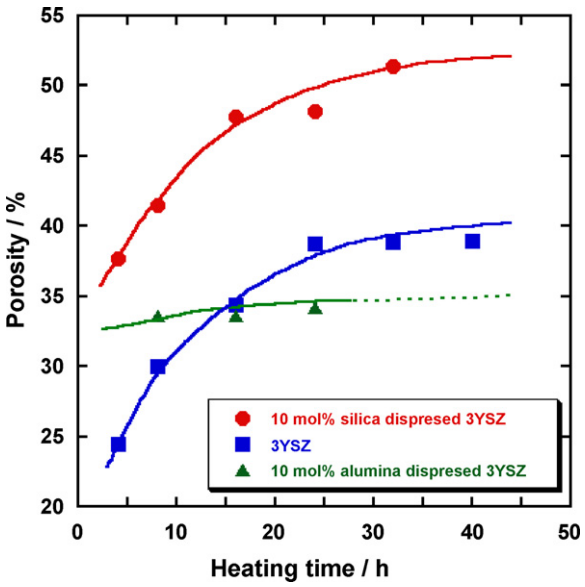

Fig. 2. Heating time dependent porosity of zirconia based ceramic foam with addition of silica or alumina.

Compared with the foam without an additive, the alumina-dispersed matrix foam had a greater porosity after 8 h of heating. Both had similar values at 16 h, and then the size relationship reversed. During pore evolution in superplasticity foaming, the gas pressure of the inner shell first increased initially with the generation of the foaming gas. This increased gas pressure drove the pore expansion. After the gas generation became saturated, the gas pressure decreased, as did the degree of pore expansion. Then, the pore expansion ceased when the gas pressure fell below the threshold stress of deformation. Accordingly, pore evolution of 3YSZ foam became saturated at a porosity of 40% or after heating for 24 h. The threshold stress is based on the superplastic deformation ability determined by the additive and microstructure.

The difference in the dependence of porosity on the heating time between silica- and alumina-dispersed foams could be explained by the deformation speed and elongation limit indicated by the previous report.[8,9] In the superplastic deformation of 3YSZ, silica enhances both the deformation speed and elongation limit. As a result, the porosity of silica-dispersed foam is greater than that without a dispersoid at any heating time. By contrast, alumina dispersion is effective for enhancing the deformation speed, but reduces the elongation limit. Consequently, alumina-dispersed foam reaches the elongation limit within a short heating time. A reduction in the deformation limit is also suggested by the cave generation that occurred only on the surface of the alumina-dispersed foam.

Subsequently, we focussed on the effect of alumina dispersion on foam evolution to elucidate the difference in porosity between 3YSZ with and without alumina. First, the appearance of the outer surface of the alumina-doped foam was quite different from the other cases; i.e., there were many visible cavities

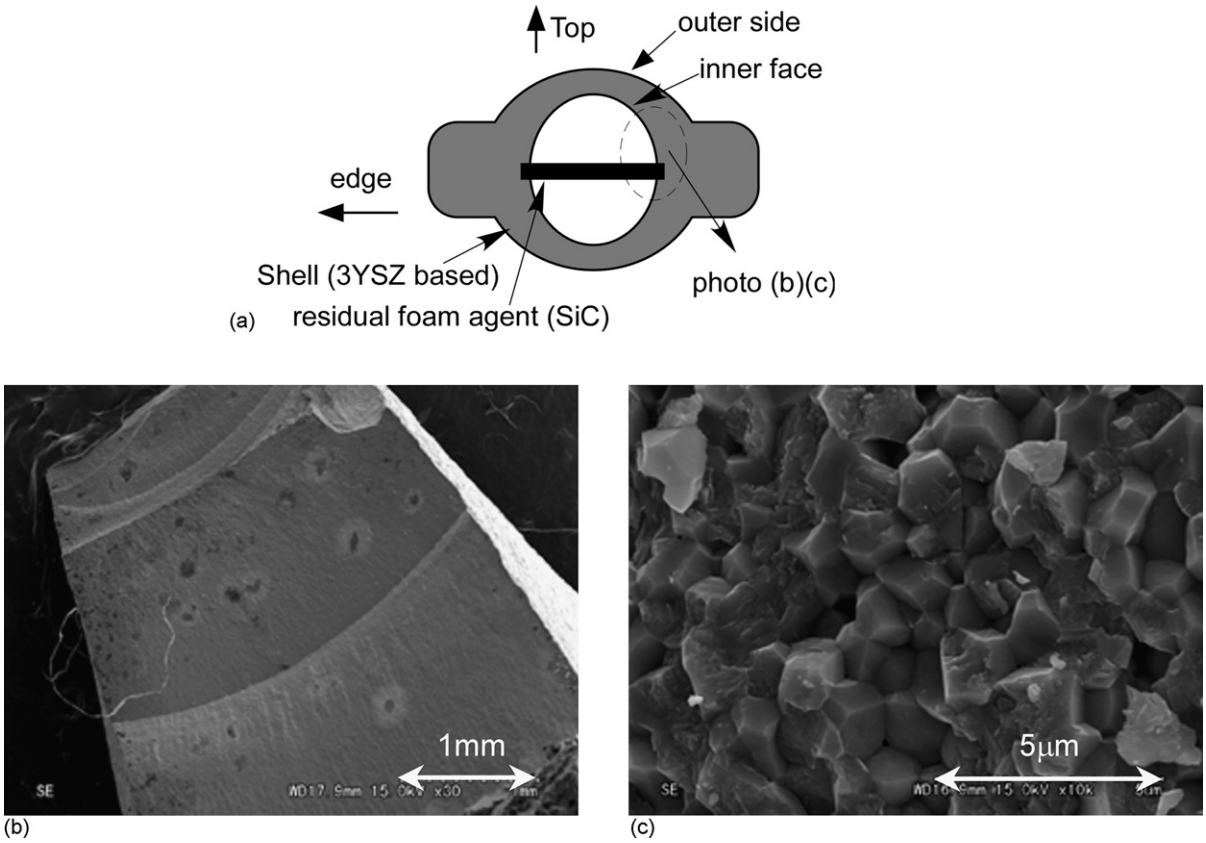

Fig. 3. Schematic illustration of sectional view (a) and SEM photos (b) and (c) of inner surface near the edge for 3YSZ mono-foams without dispersoid heat treated at 1600 °C for 8 h.

or bumps with amplitudes of less than 0.1 mm, while no such macroscopic features were seen in 3YSZ foams dispersed with silica or without dispersion.

Next, inner morphology of the foam shell was observed under an optical microscope and a SEM. Fig. 3(a) shows a photograph of the inner shell surface at low magnification for 3YSZ foams without a dispersoid. Stair-like concentric circles for which the centres coincide with the foam top are seen, suggesting the stepwise formation of pores. The high-magnification photos display a rugged morphology, like a fracture surface, as shown in Fig. 3(b). These results indicate a vestige of bonding between the 3YSZ shell and the foam agent silicon carbide (SiC). In detail, a 3YSZ matrix composite containing partially oxidised SiC was fabricated first. This bonded interface gradually exfoliated from the center with the generation of the foaming gas. As a result, the inner surface of the foam was rugged, which was different from the free surface.

Fig. 4 shows a SEM photo of the inner face at the top of 3YSZ foams heated for 4–24 h. Unlike that near the edge shown in Fig. 3(b), round grains typical of the free surface of a sintered body were observed. Since the debonding or cleavage between the matrix 3YSZ and foam agent proceeds from the center to the edge, the annealing time of the fracture surface is longer at the center (top) than at the edge. As a result, the rough surface formed during the initial stage of foaming became rounded after prolonged annealing. Furthermore, even with heating for as long as 8 h, almost all of the grains were less than 2 μm in size because the grain movement that occurred during superplastic deformation suppressed grain growth.

Fig. 5 shows a SEM photo of the inner face at the top of alumina-dispersed 3YSZ foams heated for 8–24 h. Although macroscopic caves were generated at the surface, the shell of the alumina-dispersed foam was dense. In these photos, the added alumina, which appears as dark grains, segregated at the grain boundary, especially at triple points. Compared with the foams without additives, the 3YSZ grains appeared to be slightly larger.

To examine the matrix grain growth in detail, the grain size distributions were evaluated for 3YSZ with and without alumina dispersion, and are shown in Fig. 6(a) and (b) for various heating times. In both foams, the grain distributions shifted toward the larger side with increased heating time. However, these microstructures are still characterised by small grains; *i.e.*, the largest grains are at most 5 μm, even after 24 h of heating either with or without alumina.

Fig. 6(a) shows the grain size distributions for 3YSZ foams without an additive that were heated for 4–24 h. The grain size

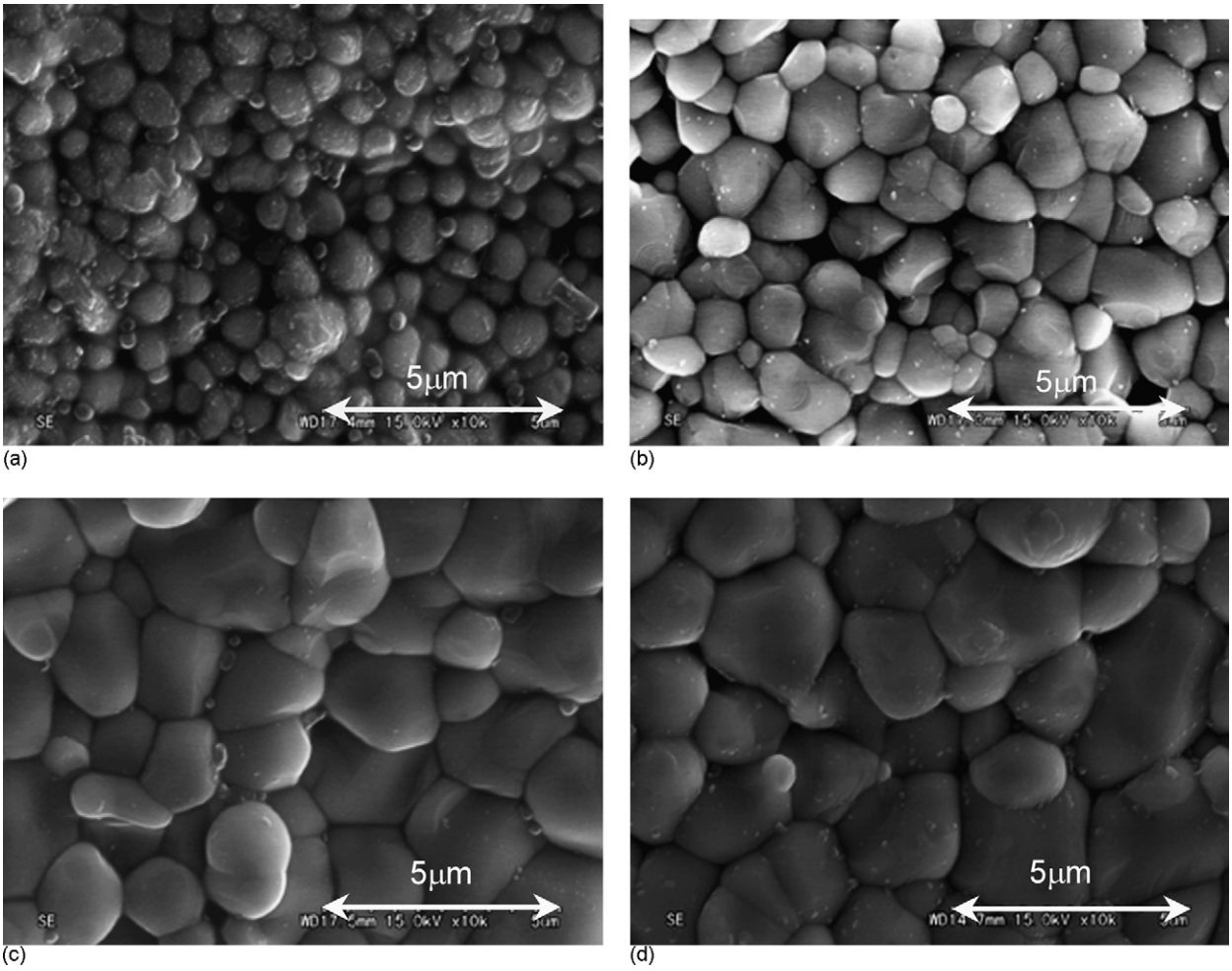

Fig. 4. SEM photos of inner surfaces at the top of 3YSZ mono-foams without dispersoid heat treated at 1600 °C for (a) 4 h, (b) 8 h, (c) 16 h, and (d) 24 h.

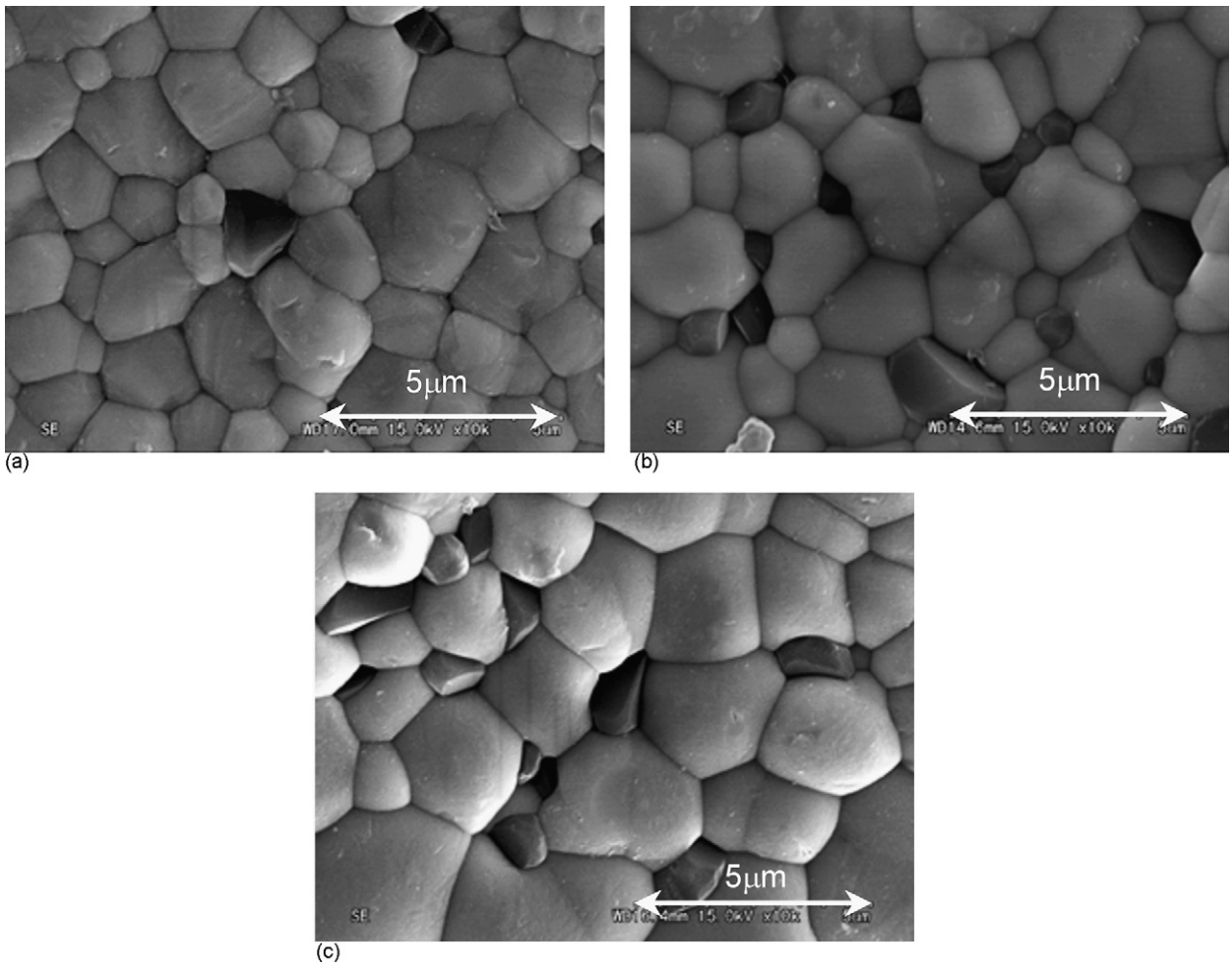

Fig. 5. SEM photos of inner surface at the top of 3YSZ mono-foams with 10 mol% of alumina heat treated at 1600 °C for (a) 8 h, (b) 16 h, and (c) 24 h.

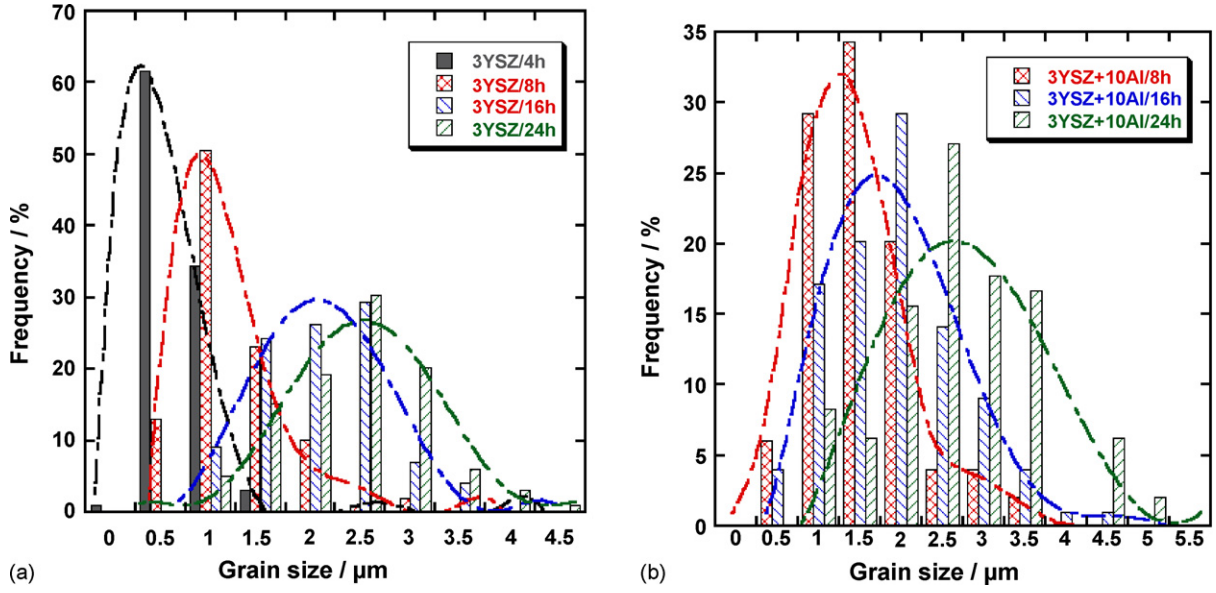

Fig. 6. (a) Grain size distributions of 3YSZ mono-foams without dispersoid heat-treated at 1600 °C for 4–24 h. (b) Grain size distributions of 3YSZ mono-foams with 10 mol% of alumina heat-treated at 1600 °C for 8–24 h.

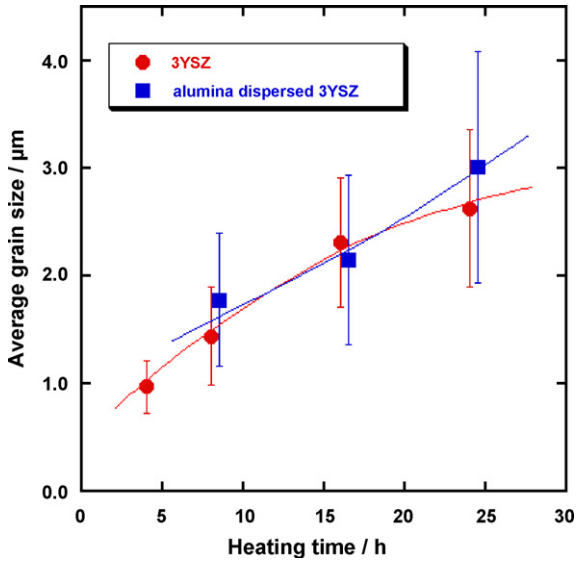

Fig. 7. Heating time dependence of average grain sizes of 3YSZ mono-foams with and without alumina. Error bar: standard deviation.

distributions are essentially unimodal at both 4 and 8 h. For the foam heated for 4 h, the grains are especially small; almost all of the grains are less than 2 μm. The pore size increases with 8 h of heating. With prolonged heating, the size distribution became broad, but still it looks unimodal.

For the alumina-doped foams, the grain size distributions were similar to those without a dispersoid, although the distribution was more complex, as shown in Fig. 6(b). Compared with the grain size distribution without a dispersoid, that for alumina-dispersed foam was shifted to slightly larger grain sizes.

The average grain sizes with and without alumina are plotted against heating time in Fig. 7. The error bars represent the standard deviation of grain size under each condition. There were no significant differences among the conditions. It is widely known that the addition of alumina frequently enhances the grain boundary density by suppressing grain growth, which facilitates grain boundary sliding.[6] In our 3YSZ-based foam, however, no significant suppression effect was seen in alumina dispersion. The foaming of alumina-dispersed 3YSZ was enhanced due to the ductility improvement that resulted from changing the state of chemical bonding at the grain boundaries, although the grain boundary density remained unchanged.

Our ceramic foams have a dense foam shell, which is equivalent to that of a standard sintered body. Recently developed methods for improving the properties of dense ceramics, such as nanocomposite formation and grain-boundary electric barrier formation, could be applied to our ceramic foam.

4. Conclusions

Zirconia-based ceramic foams were fabricated using a new superplasticity foaming method. The effects of dispersion by silica and alumina were evaluated because these compounds facilitate the 2D superplastic deformation. The porosity of the mono-foams fabricated from different matrices using the same thermal program or holding at 1600 °C for 8 h was in the order silica dispersed > alumina dispersed > without dispersoid.

The porosity of mono-foams made from 3 mol% yttria-stabilised zirconia without additives increased with heat treatment for up to 24 h and then levelled off. The porosity was greater for silica-dispersed foam than that without additives and it continued to increase for up to 40 h. Conversely, the porosity of alumina-dispersed ceramic foam reached saturation before 8 h. Consequently, the porosity of alumina-dispersed foam was greater than that without additives after heating for 8 h, while the porosity of the latter exceeded that of the former with prolonged heating for more than 16 h.

Small cavities with depths of less than 0.1 mm were seen only for the alumina-dispersed foams, while the relative densities of the foam wall exceeded 94% of the theoretical value for all three kinds of ceramic foam.

References

1. Jung, Y., Sasaki, T., Tomimatsu, T., Matsunaga, K., Yamamoto, T., Kagawa, Y. *et al.*, Distribution and structures of nanopores in YSZ-TBC deposited by EB-PVD. *Sci. Tech. Adv. Mater.*, 2003, **4**, 571–574.
2. Matsumoto, K., Itoh, Y. and Kameda, T., EB-PVD process and thermal properties of hafnia-based thermal barrier coating. *Sci. Tech. Adv. Mater.*, 2003, **4**, 153–158.
3. Diaz, A., Hampshire, S., Yang, J., Ohji, T. and Kanzaki, S., Comparison of mechanical properties of silicon nitrides with controlled porosities produced by different fabrication routes. *J. Am. Ceram. Soc.*, 2005, **88**, 698–706.
4. Kishimoto, A, Higashiwada, T., Asaoka, H. and Hayashi, H., The exploitation of superplasticity in the successful foaming of ceramics after sintering. *Adv. Eng. Mater.*, 2006, **8**(8), 708–711.
5. Kishimoto, A., Obata, M., Asaoka, H., and Hayashi, H., Fabrication of alumina-based ceramic foams utilizing superplasticity. J. Eur. Ceram. Soc., in press.
6. Hiraga, K., Morita, K., Kim, B.-N., Suzuki, S. and Sakka, Y., Microstructural design for high-strain-rate superplastic oxide ceramics. *J. Ceram. Soc. Jpn.*, 2005, **113**, 191–197.
7. Kim, B.-N., Hiraga, K., Morita, K. and Sakka, Y., A high-strain-rate superplastic ceramic. *Nature*, 2001, **413**(20), 288–291.
8. Chokshi, A. H., Nieh, T. G. and Wadsworth, J., Role of concurrent cavitation in the fracture of a superplastic zirconia–alumina composite. *J. Am. Ceram. Soc.*, 1991, **74**, 869–873.
9. Kajihara, K., Yoshizawa, Y. and Sakuma, T., The enhancement of superplastic flow in tetragonal zirconia polycrystals with SiO_2-doping. *Acta Metall. Mater.*, 1995, **43**, 1235–1242.